Cracking evolution for deep hard coal using X-ray in-situ micro-CT technology and fractal theory

Liang Zhang
Deep Mining and Rockburst Research Institute, CCTEG Chinese Institute of Coal Science, Beijing, China
State Key Laboratory Cultivation Base for Gas Geology and Gas Control, Henan Polytechnic University, JiaoZuo, China

Xiaopeng Li
Deep Mining and Rockburst Research Institute, CCTEG Chinese Institute of Coal Science, Beijing, China

Qingxin Qi
Deep Mining and Rockburst Research Institute, CCTEG Chinese Institute of Coal Science, Beijing, China

Haitao Li
Deep Mining and Rockburst Research Institute, CCTEG Chinese Institute of Coal Science, Beijing, China

ABSTRACT: Rockburst poses severe threats to the deep mining of coal mines in China; however, the fracture mechanism of deep hard coal is still unknown. Hence, this paper focuses on the cracking evolution laws for deep hard coal with high-bursting liability utilizing X-ray in-situ micro-CT technology and fractal theory. The in-situ micro-CT scanning system and bursting liability indexes for deep hard coal are first introduced in this work. Then, the uniaxial compressive experiments for the coal samples using in-situ CT scanning are conducted. Furthermore, the crack initiation, propagation, and coalescence of coal are revealed based on the in-situ micro-CT scanning experiment results. The 3D digital core of coal is obtained; four typical parameters, including fracture volume fraction and fractal dimension in 2D and 3D, are used to characterize the fracture network evolution for deep hard coal during the progressive failure process. The findings are valuable in rockburst, damage, and fracture mechanics.

Keywords: Deep mining, rockburst, hard coal, cracking evolution, in-situ micro-CT, fractal theory.

1 GENERAL LAYOUT

This manuscript contains five chapters, i.e., introduction; experiments and results; discussion; conclusions; acknowledgements; references. There are three figures, one table, and 15 references.

2 INTRODUCTION

Coal is a fundamental energy resource in China; however, with the increase in mining depth and coal demand, rockburst usually occurs during underground mining as a deadly dynamic hazard. It is reported that there are 144 coal mines facing rockburst hazards in China[1]. Even though there are considerable challenges to understanding the mechanical mechanism of rockburst, it is vital to mining safety.

Rockburst is a dynamic phenomenon that results from the sudden and violent failure of coal or rock mass, accompanied by tremendous sound. Numerous investigations have been carried out to

analyze the mechanism of rockburst, and various theories have been proposed involving the theory of strength, stiffness, energy, and bursting liability[2]. Additionally, the three primary factors theory[3], i.e., high stresses, discontinuous structure planes, and coal or rocks mechanics properties, has been proven to be one of the successful theory methods in terms of the rockburst mechanism. For coal mines in China, four mechanical parameters, including duration of dynamic fracture, elastic strain energy index, bursting energy index, and uniaxial compressive strength, have been widely used to define the bursting liability of coal. Furthermore, the control measures of rockburst, such as high-pressure coal seam infusion, drill hole destressing, and roof hydraulic fracturing, have been suggested as effective control methods by coal mine engineers in China.

Crack instability propagation and coalescence can lead to the failure of coal or rocks[4], even rockburst. In recent decades, scholars have intensively investigated the cracking evolution of coal or rocks using X-ray computed tomography (CT) technology. Yu et al.[5] carried out X-ray CT scanning experiments before the load was applied and after the backfill samples failed. They investigate the basic mechanical properties of rocks using CT scanning technology. Still, the crack and damage evolution inside coal or rocks during the entire stress-strain stages, i.e., compaction, elastic deformation, plastic deformation, and post-peak softening stages, is unclear. Hence, Tian and Han[6] conducted in-situ CT tests during uniaxial compressive experiments of concrete samples and analyzed the maximum and minimum CT numbers in different scanning sections. Gao et al.[7] studied the microcracking behaviors of thermally damaged granite during uniaxial load employing the real-time CT scanning system. The results show that both the porosity of granite and the total length of cracks increase with the load increase. Furthermore, Zhou et al.[8] researched the characterization of pore-fracture networks of coal samples using a fractal method and X-ray micro-CT employing a uniaxial compressive facility. The cross-sectional slices of the coal sample were obtained by micro-CT scanning at pre-peak stages, not including the post-peak stage. Ju et al.[9] reported the 3D fracture evolution and water migration in fractured coal with a diameter of 25 mm under variable stresses induced by fluidized mining utilizing in-situ triaxial loading and CT imaging method. Wang et al.[10] studied the 3D fracture structure evolution of cylinder coal samples with a diameter of 25 mm under uniaxial and triaxial compressive experiments using CT technology. The CT scan images show crack propagation along the mineral and coal matrix. Wang et al.[11] analyzed the microscopic structure and gas seepage properties of coal samples with a diameter of 2 mm using CT reconstruction and fractal theory. Recently, Feng et al.[12], Zhou et al.[13], and Wang et al.[14] investigated the meso-damage evolution of rocks utilizing real-time CT scanning technology. However, the mechanical influences of the initial fracture structure and mineral matrix on the cracking and damage evolution of coal or rocks are still unclear.

Despite previous documents reporting the crack and damage evolution of coal or rock materials from different perspectives, the crack initiation, propagation, and coalescence for deep hard coal with high-bursting liability have not yet been well addressed. Therefore, this work will perform compressive experiments using the in-situ micro-CT scanning system and reconstruction methods to reveal the cracking evolution laws for deep hard coal with high-bursting liability. The findings have potential in geomechanics modeling, hydraulic fracturing, and rockburst control in underground mining and tunneling.

3 EXPERIMENTS AND RESULTS

3.1 Experimental equipment and material

The uniaxial compressive experiments in the present study were conducted employing the in-situ X-ray micro and high-penetration CT system. Here, this in-situ micro-CT system was designed and assembled by the Deep Mining and Rockburst Research Institute, CCTEG Chinese Institute of Coal Science. As illustrated in Figure 1a, the in-situ micro-CT system primarily contains an X-ray source, 3D automatic hoist, and detector. The chamber held the sample, the stress was loaded at axial orientation, and the X-ray was scanned horizontally during the test. Additionally, the spatial resolution and pixel detail resolution of this CT system are two μm and 500 nm, respectively. The number of CT scanning slices imaged by this system is more than 2000 in terms of the XY plane. As

in actual practice, fractures in coal mines have an extensive range from millimeters to meters or even broader range. This in-situ micro-CT system can inspect the fractures range and samples tested from two um to 600 mm. The in-door experiments by samples tested in this paper match the micro-CT technology.

The coal bulks were cored from a deep coal mine in northern China, where the coal seams buried over 800 m. According to the standard suggested by the International Society of Rock Mechanics (ISRM)[15], the cylinder coal samples were drilled into the size of 50 mm in diameter and 100 mm in height, as shown in Figure 1b. It should be noted that the upper and lower surface of the specimens were polished to ensure that the center of gravity of the samples is vertical and avoid being bent during compression. The density, uniaxial compressive strength, Young's Modulus, and Poisson's ratio of coal samples are 1317 kg·m^{-3}, 19.15 MPa, 4.58 GPa, and 0.23, respectively. The four bursting liability indexes of coal are tested. The duration of dynamic fracture, uniaxial compressive strength, elastic strain energy index, and bursting energy index are 32.52 ms, 19.15 MPa, 18.67, and 10.71, respectively. The Chinese standard for the classification and laboratory test method on the bursting liability of coal indicates that the bursting liability of coal material tested in this study is high.

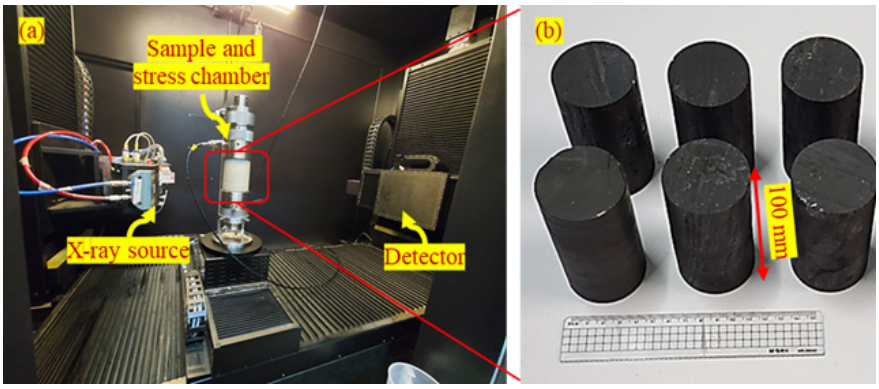

Figure 1. In-situ micro-CT system for rock mechanics testing (**a**) and coal samples prepared (**b**).

3.2 Experimental method and results

A series of uniaxial compressive experiments for coal samples was carried out. The cracking evolution properties of coal samples under different levels of axial loads were obtained using in-situ micro-CT scanning technology and reconstruction method. Five coal samples were tested in this work. There are 2185 slices in the XY direction for each sample in total, and the thickness of each slice is 0.0458 mm.

The 1200th scanning slice of sample #50-02 under each level of axial loading was analyzed in this study, as illustrated in Figure 2. The uniaxial compressive strength (σ_c) of this coal sample is 16.59 MPa. Each CT slice contains the coal matrix, cracks, and minerals. The eight scanning points at the entire stress-strain curve are 0.06σ_c; 0.12σ_c; 0.18σ_c; 0.36σ_c; 0.60σ_c; and 0.84σ_c at the pre-peak stages, 0.90 σ_c at the post-peak stage, and ultimately fractured morphology, i.e., h point, as shown in Figure 2. Each color represents different materials, i.e., the bright, black, and gray represent minerals (Figure 2a), cracks (Figure 2h), and coal matrix, respectively. Figure 2 shows that crack propagation primarily occurs at the plastic deformation stage (Figure 2f), and unstable crack propagation and coalescence mainly happen during the post-peak phase (Figures 2g and 2h). The secondary crack propagates and merges along the mineral and primary fracture tips.

4 DISCUSSION

Quantitative analysis of dynamic fracture evolution of deep hard coal with high-bursting liability, subjected to compressive loads, is of great significance to the mechanical mechanism of rockburst. This paper presents the quantitative characterization methods for discrete fracture networks in compressive experiments. Four typical parameters, i.e., 2D fracture volume fraction, 2D fracture

volume fraction, 3D fractal dimension, and 3D fractal dimension, are introduced to characterize the evolution laws of fracture networks within the deep hard coal with high-bursting liability. Here, the 2D fracture volume fraction (φ_s) is the ratio of fracture surface area (S_f) to the total surface area inner the 1200th slice (S_t). It can be defined as:

$$\varphi_s = S_f / S_t \tag{1}$$

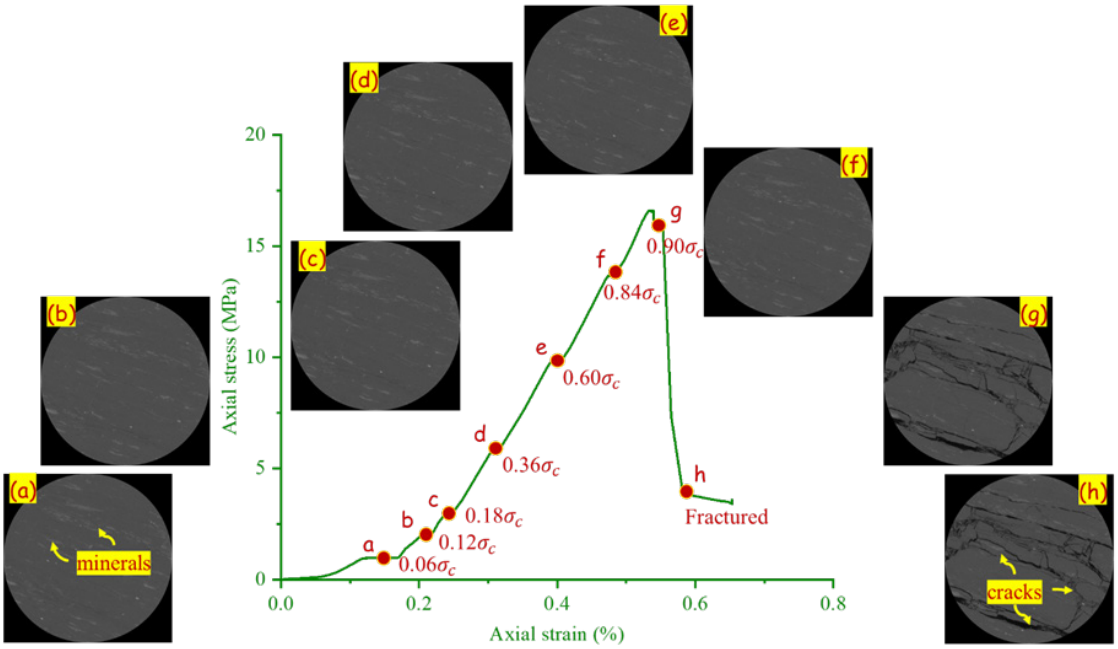

Figure 2. Entire stress-strain curve and the 1200th CT scanning slice in XY direction of deep hard coal with high-bursting liability under eight levels of compressive load.

Similarly, the 3D fracture volume fraction (φ_v) represents the ratio of all fracture networks within 2185 slices (V_f) to the total volume of the coal sample (V_t). Thus, it can be defined as follows:

$$\varphi_v = V_f / V_t \tag{2}$$

Additionally, compared with the 2D fracture volume, the 3D fracture volume fraction is more likely to be used for practical sites considering the spatial distribution of discrete fracture networks (DFNs) is three-dimensional and irregular.

Table 1. 2D and 3D fracture volume fraction and fractal dimension of deep hard coal with high-bursting liability subjected to different levels of compressive load.

Axial load	2D fracture volume fraction	3D fracture volume fraction	2D fractal dimension	3D fractal dimension
$0.06\sigma_c$	0.0083891	0.00588505	1.09552	2.06577
$0.12\sigma_c$	0.0079994 ↓	0.00556303 ↓	1.08912 ↓	2.05346 ↓
$0.18\sigma_c$	0.0145996 ↑	0.01020460 ↑	1.19179 ↑	2.17699 ↑
$0.36\sigma_c$	0.0088154 ↓	0.00604187 ↓	1.09942 ↓	2.07317 ↓
$0.60\sigma_c$	0.0089155 ↑	0.00609118 ↑	1.10764 ↑	2.07832 ↑
$0.84\sigma_c$	0.0119505 ↑	0.00803511 ↑	1.15271 ↑	2.13323 ↑
$0.90\sigma_c$	0.216596 ↑	0.154424 ↑	1.44783 ↑	2.42483 ↑
Fractured	0.170228 ↓	0.122225 ↓	1.45481 ↑	2.43527 ↑

Furthermore, the fractal dimension, one of the most critical parameters in fractal theory, is introduced to characterize the evolution of fracture networks. It is an effective indicator for quantitatively evaluating the irregularity and complexity of fracture networks. The box-counting fractal dimension

method is used to determine the fractal dimension of fracture networks. The box-counting fractal dimension can be calculated with the following formula:

$$D = -\lim_{r \to 0} \frac{\log N(r)}{\log r} \tag{3}$$

where D is the fractal dimension, r and $N(r)$ represent the side length of the cube box and the number of boxes covering the fracture networks. Hence, the fracture volume fraction and fractal dimension of the coal sample during compressive experiment can be calculated, as listed in Table 1. Moreover, the 3D model of the fracture networks inside coal is built to make the axial connectivity visualization, as shown in Figure 3.

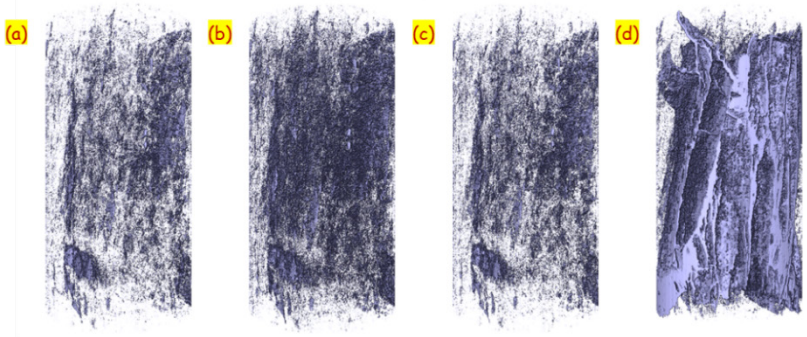

Figure 3. 3D visual model of the facture network inside deep hard coal subjected to uniaxial compressive loads: **a~d** presents the 3D fracture network of $0.12\sigma_c$, $0.18\sigma_c$, and $0.60\sigma_c$ at the pre-peak stages, $0.90\sigma_c$ at the post-peak stage, respectively.

Comparing the four parameters at $0.06\sigma_c$ and $0.12\sigma_c$ shows that the fracture networks are compacted at the stage of $0.06\sigma_c$ and $0.12\sigma_c$. For instance, the 3D fracture volume fraction and fractal dimension of the load $0.12\sigma_c$ are 0.00556303 and 2.05346, respectively, smaller than that of the load $0.06\sigma_c$. As the axial load rises to $0.18\sigma_c$, the fracture volume fraction and fractal dimension increase significantly. For example, the 3D fractal dimension increases from 2.05346 to 2.17699. It indicates that the crack growth and propagation occur at the loading level of $0.18\sigma_c$, as detailed in Figure 3b. With the axial loading level increasing from $0.36\sigma_c$ to $0.84\sigma_c$, the coal sample undergoes elastic deformation, stable crack propagation (Figure 3c), and unstable crack propagation, respectively, the fracture volume fraction and fractal dimension increase accordingly. Once the coal sample enters the post-peak stage, many fractures propagate and coalesce unstably. The 2D fracture volume fraction and 2D fractal dimension increase from 0.0119505 to 0.216596, and 1.15271 to 1.44783, respectively, as the loading level rises from $0.84\sigma_c$ (pre-peak) to $0.90\sigma_c$ (post-peak). Figure 3d shows the characteristic of crack coalescence with high connectivity when coal fractured. Additionally, as seen from Table 2, an interesting observation is that the fracture volume fraction decreases, but the fractal dimension increases with the loading level from $0.90\sigma_c$ (post-peak) to failure. It is suggested that the fracture networks of the failure point are more irregular and complex than that of $0.90\sigma_c$ (post-peak), and the volume of the coal matrix increases significantly.

5 CONCLUSIONS

According to the X-ray in-situ micro-CT scanning experiments and 3D reconstruction results, the current document focuses on the cracking evolution of deep hard coal. The following conclusions can be concluded from the experimental and calculation results.

The evolution characteristics of discontinuous structures, including cracks and minerals within deep hard coal with high-bursting liability during the progressive failure process, are revealed. Unstable crack propagation and coalescence mainly occur at the post-peak phase. The secondary crack propagates and merges along the mineral and primary fracture tips. Moreover, the high-resolution 3D digital cores of deep hard coal under different levels of compressive load are obtained.

Four typical parameters, i.e., fracture volume fraction and fractal dimension in 2D and 3D, are introduced to characterize the evolution laws of fracture networks inside the deep hard coal with high-bursting liability. With the rise in axial load, those parameters decrease at the compaction stage.

However, as the axial load increases, those four parameters increase at the elastic and plastics stages. Once it exceeds compressive strength, those four parameters increase significantly at the post-peak stage.

ACKNOWLEDGEMENTS

This work was supported by the State Key Laboratory Cultivation Base for Gas Geology and Gas Control (Henan Polytechnic University) (Grant No. WS2022B02); the Science and Technology Innovation Venture Capital Special Project of China Coal Technology & Engineering Group (Grant No. 2020-2-ZD001 and 2022-3-ZD001).

REFERENCES

[1] Dou L., Tian X., Cao A., Gong S., He H., He J., Cai W., Li X. 2022. Present situation and problems of coal mine rock burst prevention and control in China. *Journal of the China Coal Society*, 47, pp. 152-171.
[2] Jiang Y., Zhao Y., Wang H., Zhu J. 2017. A review of mechanism and prevention technologies of coal bumps in China. *Journal of Rock Mechanics and Geotechnical Engineering*, 9, pp. 180-194.
[3] Qi Q., Li Y., Zhao S., Zhao N., Zheng W., L., Li H. 2019. Seventy years development of coal mine rockburst in China: establishment and consideration of theory and technology system. *Coal Science and Technology*, 47, pp. 1-40.
[4] Zhang L., Ren T., Li X., Tan L. 2021, Acoustic emission, damage, and cracking evolution of intact coal under compressive loads: experimental and discrete element modelling. *Engineering Fracture Mechanics*, 252, pp. 107690.
[5] Yu X., Kemeny J., Li J., Song W., Tan Y. 2021, 3D observations of fracturing in rock-backfill composite specimens under triaxial loading. *Rock Mechanics and Rock Engineering*, 54, pp. 6009-6022.
[6] Tian W., Han N. 2019, Analysis on meso-damage processes in concrete by X-ray computed tomographic scanning techniques based on divisional zones. *Measurement*, 140, pp. 382-387.
[7] Gao J., Xi Y., Fan L., Du X. 2021, Real-time visual analysis of the microcracking behavior of thermally damaged granite under uniaxial loading. *Rock Mechanics and Rock Engineering*, 54, pp. 6549-6564.
[8] Zhou H., Zhong J., Ren W., Wang X., Yi H. 2018, Characterization of pore-fracture networks and their evolution at various measurement scales in coal samples using X-ray μCT and a fractal method. *International Journal of Coal Geology*, 189, pp. 35-49.
[9] Ju Y., Xi C., Wang S., Mao L., Wang K., Zhou H. 2021, 3-D fracture evolution and water migration in fractured coal under variable stresses induced by fluidized mining: In situ triaxial loading and CT imaging analysis. *Energy Reports*, 7, pp. 3060-3073.
[10] Wang D., Zeng F., Wei J., Zhang H., Wu Y. Wei Q. 2021, Quantitative analysis of fracture dynamic evolution in coal subjected to uniaxial and triaxial compression loads based on industrial CT and fractal theory. *Journal of Petroleum Science and Engineering*, 196, pp. 108051.
[11] Wang G., Qin X., Shen J., Zhang Z., Han D., Jiang C. 2019, Quantitative analysis of microscopic structure and gas seepage characteristics of low-rank coal based on CT three-dimensional reconstruction of CT images and fractal theory. *Fuel*, 256, pp. 115900.
[12] Feng X., Chen S., Zhou H. 2004, Real-time computerized tomography (CT) experiments on sandstone damage evolution during triaxial compression with chemical corrosion. *International Journal of Rock Mechanics and Mining Sciences*, 41, pp. 181-192.
[13] Zhou X., Zhang Y., Ha Q. 2008, Real-time computerized tomography (CT) experiments on limestone damage evolution during unloading. *Theoretical and Applied Fracture Mechanics*, 50, pp. 49-56.
[14] Wang P., Qiao H., Zhang Y., Li Y., Feng Q., Chen K. 2020, Meso-damage evolution analysis of magnesium oxychloride cement concrete based on X-CT and grey-level co-occurrence matrix. *Construction and Building Materials*, 255, pp. 119373.
[15] Jaeger J., Cook N., Zimmerman R. 2007, Fundamentals of rock mechanics. *Oxford: Blackwell Publishing Ltd*, 2007.